Human Rad52 Facilitates a Three-Stranded Pairing that Follows No Strand Exchange: A Novel Pairing Function of the Protein

Vasundhara M. Navadgi, Arnob Dutta, and Basuthkar J. Rao*

Department of Biological Sciences, Tata Institute of Fundamental Research, Homi Bhabha Road, Colaba, Mumbai- 400 005, India

Received June 17, 2003; Revised Manuscript Received November 1, 2003

ABSTRACT: Human Rad52 protein, by analogy with the genetics of yeast Rad52, is believed to mediate a pathway of homologous recombination even independent of Rad51. Current study is focused on unraveling the molecular properties of hRad52 that endow the protein such an ability. We show here that the hRad52 protein binds single-stranded DNA (ssDNA) as well as 3′- and 5′-tailed duplexes severalfold better than blunt-ended duplexes, altering the sensitivity of the bound DNA to the action of DNase I. Protein binding is sensitive to the length of the ssDNA: targets as short as a 33mer poorly bind the protein, whereas that of a 61mer and above bind the protein stably well. Such stable ssDNA−hRad52 complexes are highly competent in mediating not only the annealing of two complementary strands but also three-stranded pairing. The latter involves homologous recognition of linear duplex DNA by the ssDNA−hRad52 complex. We show that the hRad52 protein facilitates homologous recognition between ssDNA and duplex−DNA through a process that involves unwinding or transient unpairing of the interacting duplex via a novel three-stranded intermediate that does not lead to strand exchange. The results enable us to visualize a novel role for hRad52 that may model its function in a pathway requiring no hRad51.

Cellular DNA is subjected to damage by a variety of reactive species inside the cell and external factors such as ionizing radiation and chemical mutagens, which give rise to double-strand breaks in the genome. The double-strand breaks also arise during normal cellular events such as DNA replication, meiotic recombination, and V(D)J rearrangements. These breaks, if left unrepaired, pose a serious threat to genomic integrity. Therefore, eukaryotic cells have evolved two robust distinct pathways to repair such breaks: a high fidelity homologous recombination (HR)[1] pathway and nonhomologous end-joining (NHEJ) pathway. The choice of the repair pathways appears to be regulated developmentally, genetically, and during the cell cycle (*1*−*3*).

Genes belonging to the *RAD52* epistasis group are conserved in evolution and are shown to be involved mostly in homologous recombination events (*4*). It is now well-established that *RAD51* and *RAD52* constitute two important members of this group whose gene products exhibit ability to homologously pair DNA sequences. *Saccharomyces cerevisiae* Rad51 and human Rad51 are homologues of *Escherichia coli* RecA and promote homologous pairing and strand exchange reactions in vitro (*1*, *5*). The *RAD52* gene is conserved in yeast, humans, and mice but does not show any significant homology to the known recombination proteins in lower organisms. Despite the low sequence homology, the seven-membered ring structure of the Rad52 protein is remarkably similar to the oligomeric ring structures of *E. coli* RecT and β-protein from bacteriophage λ, all of which are competent in facilitating DNA annealing (*6*−*9*). Thus, Rad52 is believed to be a functional homologue of RecT and the β-protein. Moreover, *RAD52* stands alone as the one gene required for all homologous recombination events, only some of which also require *RAD51*. In addition, *RAD52* is involved in maintenance of telomeres in cells that lack essential components of yeast telomerase (*4*). A few recent studies point out that *RAD52* in yeast is also involved in influencing NHEJ pathway events (*10*−*12*).

Mechanistic basis of cooperation between various proteins belonging to the *RAD52* epistasis group is becoming clear through various biochemical studies. Rad52 is shown to interact with Rad51 (*13*) and replication protein A (RPA) (*14*−*16*). Rad51 and Rad52 colocalize in distinct nuclear foci in response to DNA damage (*17*). Both yeast and human Rad52 stimulate Rad51 mediated strand exchanges (*18*−*21*). Rad52 is shown to displace RPA and assist the loading of Rad51 onto ssDNA with the help of the Rad55/Rad57 heterodimer (*22*−*24*). Rad52 mediated annealing of ssDNA is stimulated by RPA supposedly via specific protein−protein interactions (*25*, *26*). In addition to strand annealing, hRad52 has been shown to promote homologous pairing between ssDNA and superhelical dsDNA substrates giving rise to D-loop formation (*27*−*29*).

Recent hRad52 crystal structure of a conserved catalytic N-terminus domain revealed a 11-subunit oligomeric ring (*29*, *30*) as opposed to a seven-subunit ring inferred from electron microscopic image reconstruction studies of full-length hRad52 protein (*7*). The crystal structure showed no basic amino acids in the central channel of the ring, but rather showed amino acids on the outside of the ring that forms a

* To whom correspondence should be addressed. Fax: 91-22-22804610, 22804611. Phone: 91-22-22804545 Ext. 2606. E-mail: bjrao@tifr.res.in.

[1] Abbreviations: 2AP, 2-aminopurine; dsDNA, double-stranded DNA; DNase I, deoxyribonuclease I; hRad52, human Rad52; HR, homologous recombination; NHEJ, nonhomologous end joining; ssDNA, single-stranded DNA.

10.1021/bi0350452 CCC: $25.00 © 2003 American Chemical Society
Published on Web 12/03/2003

Table 1: List of Oligonucleotides[a]

Name	Sequence (from 5' to 3')	Length (bases)
GCL	ggcttagagcttaattgctgaatctggtgc**tcgcctgataaattgtgtcgaaatccgcgacctgctccat gttacttagccggaacgaggc**ggattcgcgattccttgatgcctatggtga	121
CLL	tcaccataggcatcaaggaatcgcgaatccgcctcgttccggctaagtaacatggagcaggtcgcggatt tcgacacaatttatcaggcgagcaccagattcagcaattaagctctaagcc	121
Gce	**tcgcctgataaattgtgtcgaaatccgcgacctgctccatgttacttagccggaacgaggc**	61
Cle	gcctcgttccggctaagtaacatggagcaggtcgcggatttcgacacaatttatcaggcga	61
W78	aacggagatttgtatca**tcgcctgataaattgtgtcgaaatccgcgacctgctccatgttacttagccg gaacgaggc**gcaga	83
W58C	taaattgtgtcgaaatccgcgacctgctccatg	33
3T-CLL	aattgtgtcgaaatccgcgacctgctccatgttacttagccggaacgaggcggattcgcgattccttgatg ctatggtga	81
5T-CLL	ggcttagagcttaattgctgaatctggtgctcgcctgataaattgtgtcgaaatccgcgacctgctccatgtt acttagcc	81
PUC	tttcccagtcacgacgttgtaaaacgacggccagtgccaagcttgcatgcctgcaggtcgactctagagg atccccgggtaccgagctcgaattcgtaatcatggtcatagctgtttcct	120
T-template	acgcacatactaggctgtatttttttttttttttttttttttttttttttttcagtacagtcatgacagt	70
A-template	actgtcatgactgtactgaaaaaaaaaaaaaaaaaaaaaaaaaaaaaaaaaaaatacagcctagtatgtgcgt	70
2AP-A template	actgtcatgactgtactgaaaaaaaaaaaaaaaa**x**aaaaaaaaaaaaaaaaaatacagcctagtatgtgcgt	70
A60	aaaaaaaaaaaaaaaaaaaaaaaaaaaaaaaaaaaaaaaaaaaaaaaaaaaaaaaaaaaaaaaaaaaaaaaaa	60
2AP-A60	aaaaaaaaaaaaaaaaaaaaaaaaaaaaaa**x**aaaaaaaaaaaaaaaaaaaaaaaaaaaaaaaaaaaaaa	60
T60	tttttttttttttttttttttttttttttttttttttttttttttttttttttttttttttttttttttttttt	60

[a] W58C sequences present in GCL, Gce, and W78 are underlined. Gce sequences present in GCL and W78 are shown in bold. X denotes 2-amino purine in oligonucleotides 2AP-A template and 2AP-A60.

positively charged surface for DNA binding, which was confirmed by mutation studies of the residues in DNA binding sites. Keeping this model in view, where a positively charged groove on the surface of the ring lodges binding sites for both single as well as dsDNA, we tested a mechanistic issue related to hRad52 mediated three-stranded pairing. We show that the ssDNA−hRad52 complexes are competent in promoting three-stranded pairing, where hRad52 facilitates homologous recognition between ssDNA and linear duplex−DNA through a process that involves transient unpairing of the interacting duplex via a novel intermediate that is not followed by the imminent strand exchange.

MATERIALS AND METHODS

Materials. T4 polynucleotide kinase, DNase I, and Q-sepharose were purchased from Amersham Life Sciences. PMSF, BSA, and glutaraldehyde were purchased from Sigma. Ni-NTA agarose beads were purchased from Qiagen. Oligonucleotides were obtained from DNA technology (Denmark).

DNA Substrates. All oligonucleotides were purified on denaturing polyacrylamide gels and desalted, as described (*31*, *32*). The purity of an oligonucleotide was judged by ^{32}P labeling at the 5′-end by T4 polynucleotide kinase, followed by analysis on a 10% denaturing polyacrylamide gel, which revealed that they were more than 90% pure. The DNA substrates used in this study are listed in Table 1. All DNA concentrations are expressed in nucleotides.

End Labeling of Oligonucleotides. Oligonucleotides were end labeled by T4 polynucleotide kinase and [γ-^{32}P] ATP, as described (*31*).

DNA Annealing. Annealing reactions were done in a 10 μL volume with equimolar concentrations of both strands in 10 mM Tris-HCl (pH 7.5) and 5 mM $MgCl_2$. Samples were heated at 90 °C for 5 min and slow cooled to room temperature. Completion of annealing was assessed by analysis on native polyacrylamide gel (PAGE), which showed that all of the labeled strand was converted to duplex. Completion of annealing between unlabeled strands was assessed by 5′-end labeling an aliquot of the duplex with [γ-^{32}P] ATP, followed by analysis on a native PAGE, which showed no residual ssDNA.

Purification of hRad52. The hRad52 overexpressing clone was obtained from Steve West (Cancer Research UK, earlier ICRF). Protein was purified as described (*18*) with the following changes. Supernatant obtained following a high-speed centrifugation of cell lysate (from a 4 L culture) was mixed gently for 1 h at 4 °C with 4 mL of Ni-NTA-agarose beads that were preequilibrated in 20 mM Tris-HCl (pH 8.0), 0.5 M NaCl, 10% glycerol, 0.02% Triton X 100, 0.2 mM phenyl methyl sulfonyl fluoride (PMSF), and 5 mM imidazole. Following such batch incubation, the beads were packed into an Econo-column (Bio-Rad) and washed, and hRad52 was eluted as described for the talon column (*18*). Fractions containing hRad52 were pooled; dialyzed against 20 mM Tris-HCl (pH 8.0), 50 mM KCl, 1 mM EDTA, 0.5

mM dithiothreitol (DTT), 10% glycerol, 0.2 mM PMSF; and loaded onto a 10 mL Q-sepharose column that was pre-equilibrated with the same buffer. The bound proteins were eluted by a gradient of 50−500 mM KCl in the previous buffer. Fractions containing pure hRad52 (as analyzed by silver-stained SDS−PAGE) were pooled, dialyzed, and stored in 20 mM Tris-HCl (pH 8.0), 50 mM KCl, 0.5 mM EDTA, 1 mM DTT, 50% glycerol, and 0.05 mM PMSF. hRad52 thus obtained was found to be free of any nuclease contamination.

DNA Binding by Gel-Shift Assays. Labeled DNA substrate was incubated with various concentrations of hRad52 (as described in the figure captions) in a binding buffer [30 mM Tris-acetate (pH 7.5), 1 mM $MgCl_2$, 1 mM DTT, and 100 μg/mL BSA] at 37 °C for 10 min. Rad52−DNA complexes were fixed with glutaraldehyde (0.2%) for 20 min at 37 °C, followed by analysis on 8% native PAGE in TBE buffer at 200 V for 3 h (∼25 °C). The gels were dried, and the radioactivity was quantified by ImageQuant software on a PhosphorImager (molecular dynamics).

DNase I Assays. hRad52 binding with the labeled DNA was performed as described previously for gel-shift assays. The protein−DNA complexes (10 μL) were allowed to attain room temperature for few minutes and were treated with 2 μL of DNase I at room temperature for 2 min. Final concentration of DNase I used in the case of ssDNA and double-tailed duplex was 0.325 ng/μL (8.1×10^{-4} units/μL), and for dsDNA, it was 0.16 ng/μL (4×10^{-4}units/μL). The digestion reaction was stopped by adding formamide (50%), SDS (0.5%), and EDTA (10 mM). The samples were heat denatured at 90 °C for 5 min, quick-chilled, and electrophoresed at 50 °C on a 10% denaturing polyacrylamide gel containing 6 M urea. The gels were dried followed by autoradiography.

Three-Stranded Pairing Assay. Indicated amounts of hRad52 was allowed to bind to ssDNA (2.0 μM) in the binding buffer at 37 °C for 10 min (as described previously in the gel-shift assay). Pairing was initiated by the addition of the labeled duplex (1.0 μM) and 10 mM $MgCl_2$, followed by incubation for another 10 min. The complexes were fixed with glutaraldehyde (0.2%) for 20 min at 37 °C. The samples were analyzed by both 8% native PAGE as well as by filter binding assay as described (*33*).

Strand Exchange Activity. Three-stranded pairing was done as described previously. To observe the strand exchange products, the samples were deproteinized with SDS (0.5%), EDTA (10 mM), and proteinase K (500 μg/mL) by incubating at 37 °C for 20 min and subjected to electrophoresis on 8% native gel. The release of the labeled ssDNA was quantified using ImageQuant software on a PhosphorImager (molecular dynamics).

Fluorescence Measurements. The steady state fluorescence measurements were carried out by using a SPEX fluorolog FL1T11 spectrofluorometer as described earlier (*34*). Fluorescence emission scans of 2AP containing substrates showed a clear emission maximum at 370 nm following an excitation at 310 nm. So in all experiments, 2AP fluorescence was monitored in a reaction (250 μL of binding buffer described for gel-shift assay) at 25 °C by exciting at 310 nm and measuring the emission at 370 nm. All fluorescence intensities were corrected for variable background emissions and lamp fluctuations (signal/reference: s/r). Hence, all fluorescence intensities are plotted as s/r values.

RESULTS

Although it has been shown that hRad52 is proficient in strand annealing and D-loop formation, comparative details of protein binding to various forms of DNA (ssDNA, blunt-ended duplex, and tailed duplexes) and the competence of such hRad52−DNA complexes in bringing about a three-stranded pairing with the linear duplex are unclear. We have tried to study these aspects in the current paper.

hRad52 Binding to DNA. We used two independent assays to monitor the binding. The first assay monitored the DNA with respect to its sensitivity/protection to DNase I as a function of hRad52 protein concentration.. The second assay measured the formation of hRad52−DNA complexes in a gel-shift analysis.

DNase I Probing Assay. Three different DNA substrates were used: ssDNA, blunt-ended duplex, and tailed duplex. In all the cases, the common strand (121mer, GCL) was 5′-end labeled with γ-^{32}P ATP. Annealing the labeled strand with either an unlabeled complementary full-length strand (121mer, CLL) or a shorter length strand (61mer, Cle) yielded the blunt-ended and the tailed duplexes, respectively. In the latter case, annealing ensued in the middle of GCL, generating a duplex with nearly equal lengths of 3′- and 5′-tails (30mers) in the tailed duplex molecule. Annealing was performed at 1:1 ratio of labeled to unlabeled strands where duplex formation was complete as analyzed by native PAGE analysis (data not shown). Since a common strand is uniquely labeled in all three substrates, analyses of this strand with respect to DNase I sensitivity/protection as a function of the hRad52 protein concentration would reveal a relative comparison of protein binding on these three different DNA substrates. In the case of ssDNA, the addition of protein led to accentuated digestion of the strand by DNase I (Figure 1A). In the same set of conditions when DNase I was omitted, the addition of hRad52 did not result in digestion of DNA strand (Figure 1E). Even at the highest concentration of protein, no strand nicking was evident, suggesting that the hypersensitivity to DNase I in the presence of hRad52 was due to the hRad52 induced structural change in the DNA rather than a spurious nicking activity in purified hRad52 preparation. A similar hypersensitivity was observed with tailed duplexes (Figure 1C). Again, a control without DNase I revealed no nicking as a function of hRad52 protein concentration (data not shown). The extent of hypersensitivity observed in the ssDNA versus tailed duplexes, as a function of hRad52 concentration, was measurably different: while a low concentration (0.5 μM) of hRad52 induced a significant level of hypersensitivity in ssDNA, such an effect was hardly visible with the tailed duplex. At the next higher concentration (1.0 μM) of the protein, the hypersensitivity in ssDNA increased further and remained so even at a higher concentration of protein. On the contrary, tailed duplexes exhibited hypersensitivity only at a higher (1.0 μM) concentration of protein and showed a gradual increase as a function of protein concentration. In the same experiment, across the entire range of protein concentrations tested, we observed no changes in the DNase I sensitivity status of the duplex DNA (Figure 1B). To assess whether the nicking pattern in the ssDNA/tailed duplex DNA following hRad52 binding reflected the

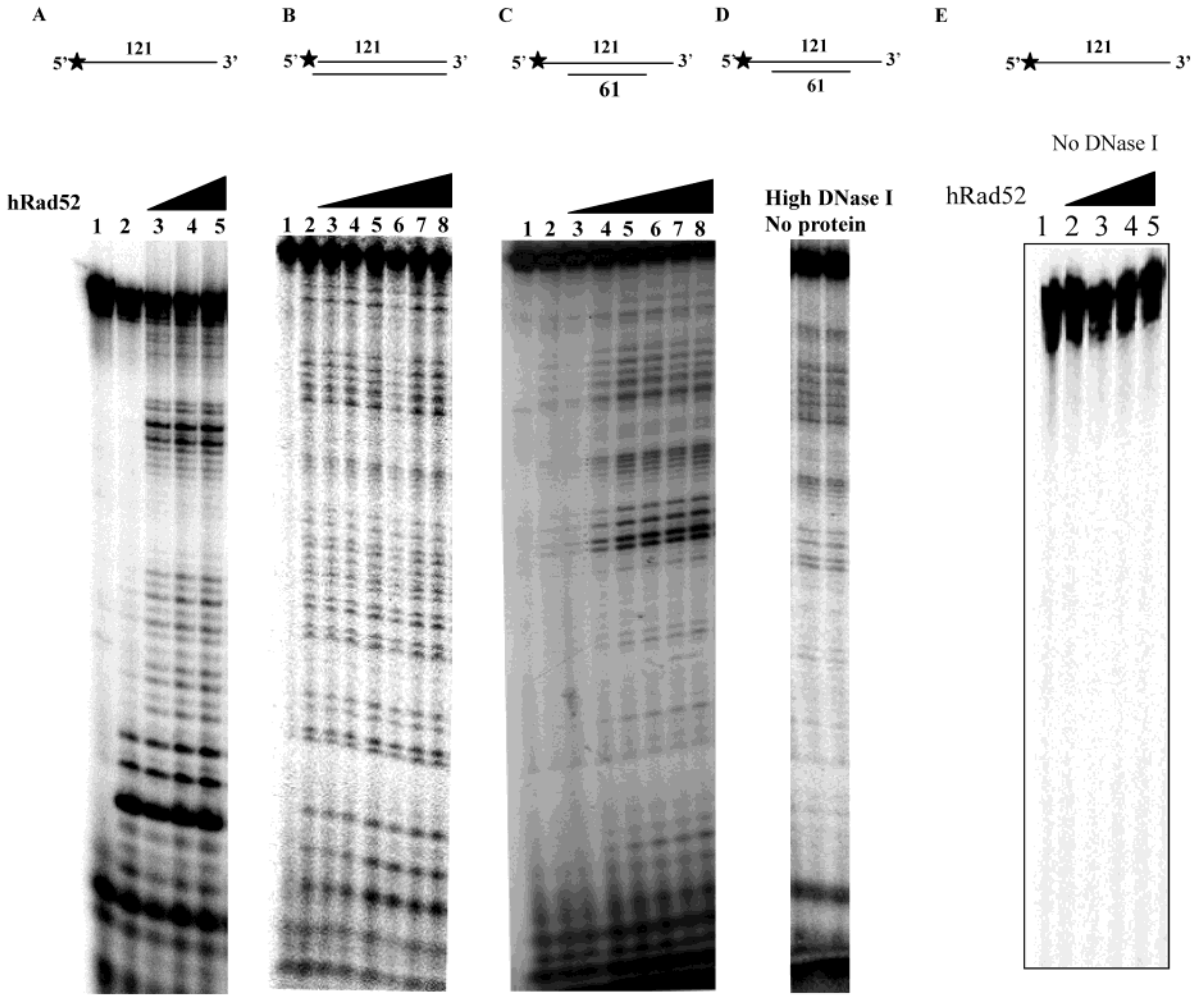

FIGURE 1: DNA binding properties of hRad52: DNase I probing assay. (A) ^{32}P labeled GCL ssDNA (1.0 μM) or (B) ^{32}P labeled GCL annealed with unlabeled complementary CLL (1.0 μM each, blunt-ended duplex) or (C) ^{32}P labeled GCL annealed with unlabeled complementary Cle (1.0 μM, double tailed duplex) were incubated with increasing concentrations of hRad52, followed by DNase I probing analyses (0.325 ng/μL for ssDNA and double-tailed duplex and 0.16 ng/μL for dsDNA) (see Materials and Methods). Lane 1 in panels A−C contains samples where neither hRad52 nor DNase I was added. The samples in all the remaining lanes were DNase I treated. In panel A, lanes 2−5 contain 0, 0.5, 1.0, and 1.5 μM hRad52, respectively. In panels B and C, lanes 2−8 contain 0, 0.5, 1.0, 1.5, 2.0, 2.5, and 3.0 μM hRad52, respectively. (D) Naked double-tailed duplex samples treated with a higher concentration of DNase I (0.8 ng/μL). (E) Samples same as in panel A but without any DNase I treatment. Star in the cartoons indicates the ^{32}P labeled 5′ end.

intrinsic cutting pattern of the DNA, we checked the digestion at a very high DNase I concentration in the absence of hRad52. This control showed that the nicking pattern induced in the hRad52−DNA complexes was very similar to that induced in naked DNA with high DNase I (data shown only for tailed duplex, Figure 1D). This experiment revealed that the hRad52 binding to DNA results in conformational changes in DNA such that its intrinsic nicking pattern can be accentuated even at significantly lower level of DNase I, the level at which naked DNA is hardly digested. We discuss the significance of this structural transition later (see Discussion).

Mobility-Shift Assay. To verify whether the differential effects of the three DNA substrates observed in the DNase I probing assay were directly a consequence of hRad52 binding or not, we analyzed binding by a classical mobility-shift assay. Visualization as well as the quantification of the mobility-shifted DNA band corroborated the results obtained in the DNase I probing assay (Figure 2). Across a range of protein concentrations tested, while ssDNA and tailed duplexes yielded a significant level of gel-shifted complexes (Figure 2A,C), binding with blunt-ended duplexes was barely evident (Figure 2B). PhosphorImager quantitation clearly revealed this contrast where by 1−2 μM protein most of ssDNA and tailed duplex DNA was gel-shifted, less than 20% of the blunt-ended DNA was converted to gel-shifted complexes (Figure 2D). Moreover, the analyses revealed that, as in DNase I probing, essentially all ssDNA was covered by protein at a low concentration (1.0 μM) of hRad52, whereas tailed duplexes required a graded addition of higher protein levels (Figure 2D). Both these experiments put together suggest that hRad52 exhibits a differential binding affinity toward ssDNA, tailed duplex DNA, and blunt-ended duplex DNA.

To reassess the protein binding affinity difference between single-strand and double-stranded DNA more directly, we performed a competition assay. In the competition experiment, we studied the binding of hRad52 with labeled ssDNA (GCL, 121mer) (the strand used in the earlier experiment) in the presence of a molar excess of unlabeled competitor DNA. Two types of competitor DNA were used: ssDNA that was used as labeled substrate and its duplex version.

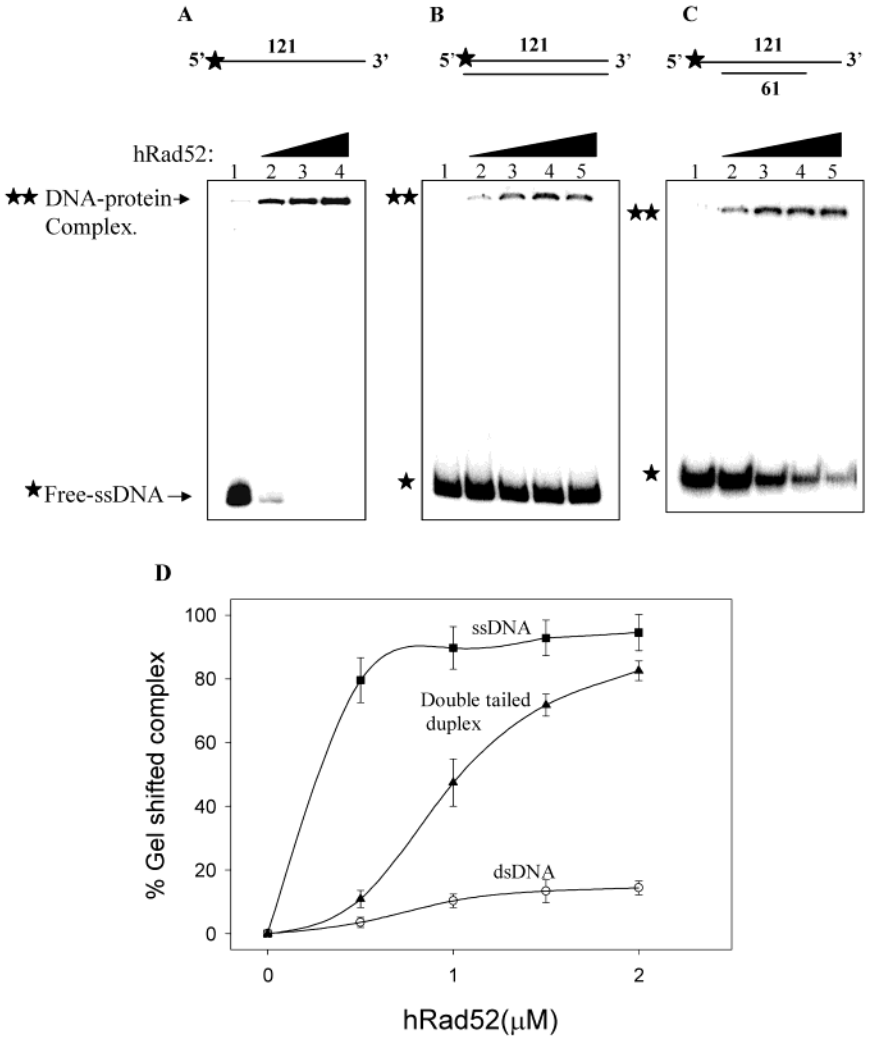

FIGURE 2: DNA binding properties of hRad52: gel-shift assay. (A) ssDNA, (B) blunt-ended, and (C) tailed duplex substrates (1.0 μM each strand) (the same as in DNase I assay) were incubated with 0, 0.5, 1.0, 1.5, and 2.0 μM hRad52 (lanes 1−5), followed by gel-shift assay (Materials and Methods) (panel A has only lanes 1−4). The positions of free DNA (★) and hRad52-DNA complexes (★★) are indicated. (D) Radioactivity associated with hRad52-DNA complexes was expressed as a percentage of total in each lane and plotted against respective hRad52 concentration. [ssDNA (■), blunt-ended duplex (○), and tailed duplex (▲)].

The competitor duplex was generated by annealing the GCL strand with the equimolar CLL strand, both in unlabeled form. Assessment of annealing efficiency as measured by labeling a small aliquot of the annealed mixture by native PAGE revealed that the sample essentially contained annealed duplexes, and no traces of free single strands were observed (data not shown). The concentrations of the labeled GCL strand as well as hRad52 were so chosen (1.0 μM each) that at this condition essentially all of the labeled DNA was gel-shifted (see Figure 2D). The addition of the molar excess (2×, 4×, 8×, 16×) of competitor DNA in the binding mixture resulted in a dose dependent decrease in labeled gel-shifted complexes (Figure 3). Concomitant with the loss of the gel-shifted complexes was the appearance of unbound labeled DNA. PhosphorImager estimation of the gel-shifted complex as a function of competitor dose revealed that the single strand is a much better competitor than the double strand. In fact, about a 16-fold molar excess of the double strands were required to achieve 50% loss of labeled gel-shifted complexes, whereas a similar loss was brought about by 1−2-fold of the ssDNA competitor. Thus, this experiment strongly corroborated the earlier one (Figure 2D) in establishing that hRad52 binds ssDNA at least an order of magnitude better than dsDNA.

It is relevant to point out that the tailed duplex employed in the earlier experiment had both 3′- and 5′-tails in the same substrate. Therefore, it was not clear which end of the duplex contributed to the higher affinity of hRad52 binding as compared to that of the duplex. To study this, we generated 3′- and 5′-tailed duplexes by annealing a labeled common strand (CLL, 121mer) with 81mer oligonucleotide that is complementary to CLL either at 5′- or 3′-end (3T-CLL and 5T-CLL, respectively). In either case, annealing results in the generation of an 81 base pair duplex with either a 3′- or 5′-overhang of 40 nucleotides in length. Analysis of the annealed duplexes on native PAGE revealed that annealing had gone to completion, and no traces of free single strands were observed. Labeled 5′- or 3′-tailed duplexes were incubated with increasing concentrations of hRad52 followed by gel-shift analysis. The experimental conditions followed were identical to that described in Figure 2. The extent of the gel-shift as a function of protein concentration for 3′- and 5′-tailed duplexes was very similar to each other as well as to that of a double-tailed duplex studied earlier (data not

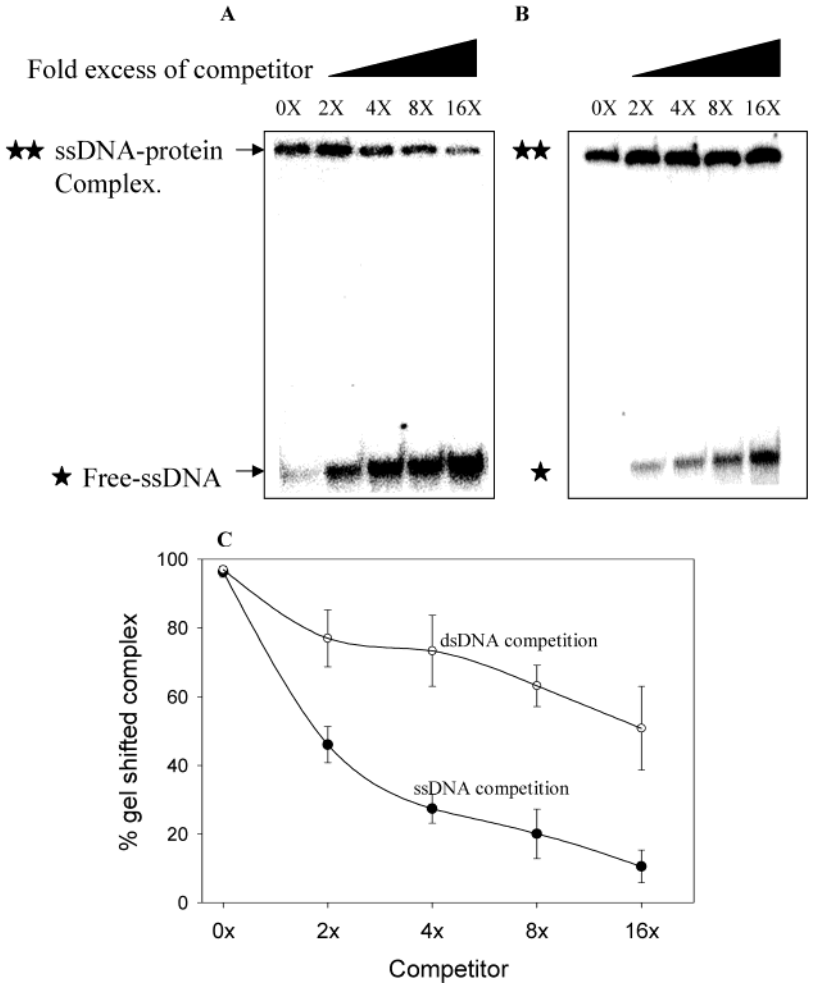

FIGURE 3: hRad52 binding to ssDNA vs dsDNA: a competition gel-shift assay. ^{32}P labeled GCL (1.0 μM) was incubated with hRad52 (1.0 μM) in the presence of either (A) unlabeled GCL or (B) unlabeled GCL/CLL duplex competitor taken at 0, 2, 4, 8, or 16 molar fold excess over that of the labeled strand, followed by gel-shift analyses. Free ssDNA (★) and the gel-shifted ssDNA−protein complex are indicated (★★). (C) The radioactivity associated with the labeled ssDNA−protein complexes (★★) was expressed as a percentage of total radioactivity in each lane and plotted against the respective fold excess of the competitor [ssDNA−competitor (closed circles); dsDNA−competitor (open circles)].

shown). Quantitation revealed that both 3′- and 5′-tails were equally competent in promoting hRad52 binding where most of the DNA was gel-shifted by an amount of hRad52 (1.5−2.0 μM) that is similar for the double-tailed duplex as well.

Effect of ssDNA Length on hRad52 Binding. Mobility-Shift Assay. As a prelude to studying three-stranded pairing mediated by hRad52, we wanted to establish the minimum length of ssDNA that is efficient in forming a stable presynaptic complex. Pairing complexes mediated by such minimal length presynaptic complexes can then be more rigorously characterized. It was clear from the previous experiments (Figures 1 and 2) that the 121mer ssDNA is efficiently bound by hRad52. In the following experiment, we wanted to assess whether single strands much shorter than the 121mer can also bind the protein well. A set of oligonucleotides, which are sequentially truncated versions of GCL (as explained in Figure 4A), was used. Such a design is likely to minimize any differential contribution of sequence context and secondary structural effects by the oligonucleotides since they share common sequences. A mixture of these four oligonucleotides (1.0 μM each expressed in nucleotide concentration) was kinased, followed by binding with an increasing concentration of hRad52. Analysis of the binding mixtures by a gel-shift assay revealed the appearance of hRad52−DNA complexes with concomitant reduction in the level of free labeled DNA (Figure 4B). In this protocol, one can clearly assess the relative binding affinity of various strands by monitoring the drop in the level of free DNA in the gel. Each of these oligonucleotides when complexed with hRad52 should yield gel-retarded species that may not be resolved from one another and hence comigrate in the gel. One can estimate the free DNA associated with each oligonucleotide and express the same as the percentage of its input DNA taken as 100%. In this analysis, varying kinasing efficiencies of different oligonucleotides are normalized because the radioactivity associated with the free DNA of each species is taken as 100% (lane 1, Figure 4B). We estimated the percentage of DNA converted to hRad52−DNA complexes by subtracting the level of leftover free DNA from 100%. When such data was plotted against the protein concentration, the effect of the DNA length dependence on protein binding was evident (Figure 4C). We saw hardly any hRad52 binding to the 33mer oligonucleotide. Protein binding essentially saturated at 4.0 μM with the 121mer, whereas a similar level of binding was reached with the 61- and 83mer only at a higher protein concentration (more than 8.0 μM). This experiment showed that in the micromolar range of protein concentration, DNA strands that

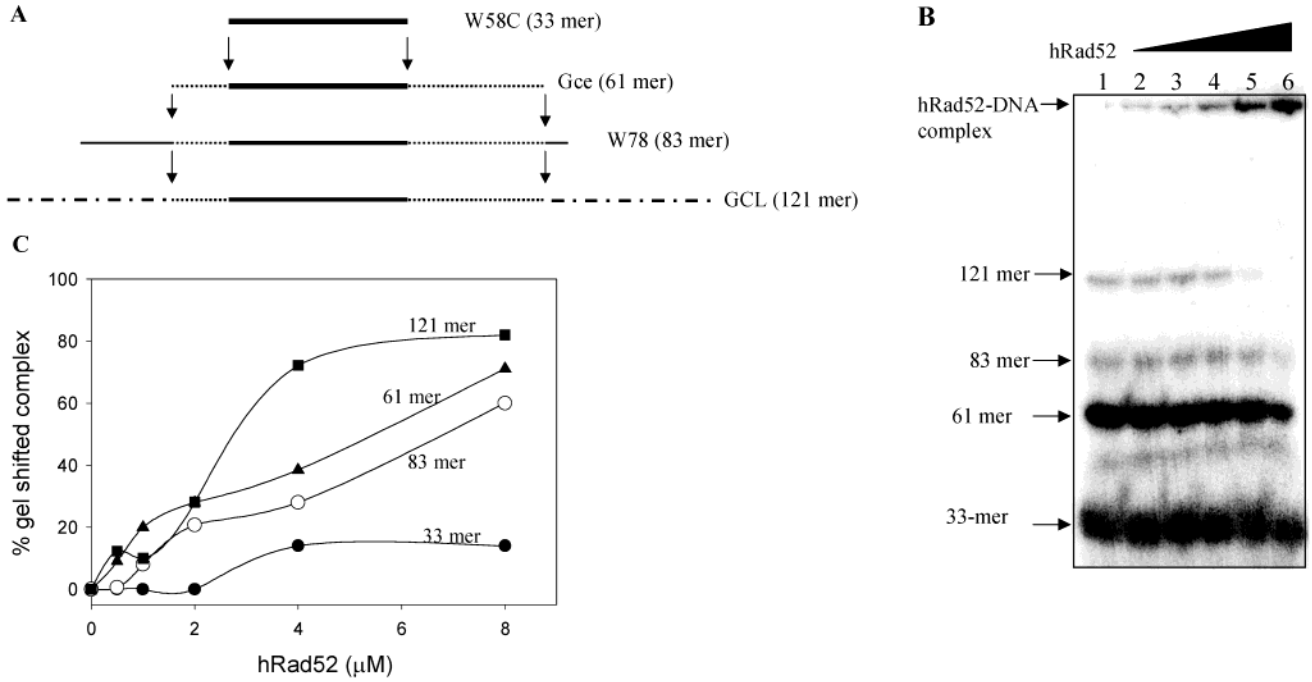

FIGURE 4: ssDNA length dependence of hRad52 binding: a gel-shift assay. (A) The schematic explains the hierarchy of oligonucleotides used. Top shorter oligonucleotide is part of the next longer one shown immediately below (in the region between arrows). Sequence stretches that are identical in different oligonucleotides are depicted by a similar line pattern. Names and lengths of oligonucleotides are indicated (see Table 1). (B) GCL (121mer), W78 (83mer), GCe (61mer), and W58C (33mer) oligonucleotides, taken as a mixture (1.0 μM each), were labeled with ^{32}P at 5′-ends, incubated with increasing concentration of hRad52 (lanes 1−6 correspond to 0, 0.5, 1.0, 2.0, 4.0, and 8.0 μM, respectively), followed by gel-shift analyses (Materials and Methods). Radioactive bands corresponding to hRad52−DNA complexes and free DNA substrate are indicated. (C) Radioactivity associated with each free substrate DNA (first lane containing no hRad52) is considered as 100%, with respect to which the free DNA in the other lanes (containing hRad52) is calculated as a percentage. DNA in gel-shifted complexes is inferred by subtracting this value from 100% and plotted against the protein concentration.

are either 61mer or longer can be efficiently bound by protein, and the binding to the 33mer is poor. Hence, in the experiments described next where we monitor hRad52-mediated DNA pairing, we used ssDNA that is a 61mer or above to generate stable hRad52−DNA complexes.

DNase I Probing Assay. hRad52 binding to a long ssDNA (121mer) had revealed a clear signature of DNase I hypersensitivity (Figure 1). Does the ssDNA length dependent binding of hRad52, as revealed in gel-shift analyses, also manifest in DNase I hypersensitivity effects? To study this aspect, we repeated DNase I probing of hRad52 complexes generated with varying length ssDNA substrates (33-, 61-, 83-. and 121mer) used in the last experiment (Figure 4). In addition, tailed duplexes carrying either a 3′- or a 5′-40mer ssDNA tail were also compared. As described earlier in the text, these 3′- and 5′-tailed duplexes were generated by annealing a labeled common strand (CLL, 121mer) with an unlabeled 81mer oligonucleotide that is complementary to CLL either at 5′-end or 3′-end (3T-CLL and 5T-CLL), respectively. As described earlier, the tailed duplex preparations were free of ssDNA contaminations and were equally competent in promoting hRad52 binding. Varying length ssDNA and 3′- and 5′-tailed duplexes (all ^{32}P labeled at the 5′-ends) were incubated with increasing amounts of hRad52, followed by DNase I probing analyses on denaturing gels. As expected, the 121mer strand showed a clear hRad52 binding dependent hypersensitivity pattern very similar to that observed earlier (Figure 1A). The DNA strand was rendered hypersensitive to DNase I even at a low concentration of hRad52 (0.5−1.0 μM) and remained so when the protein concentration was increased further (data not shown). Again, 5′-tailed as well as 3′-tailed duplexes revealed a similar and Rad52 protein concentration dependent DNase I hypersensitivity pattern (only 5′-tailed duplex data is shown) (Figure 5D). However, the relationship between ssDNA length dependent hRad52 binding and hypersensitivity was not as clear with other ssDNA substrates tested in this experiment. There was no hRad52 concentration dependent graded enhancement in DNase I hypersensitivity (of the type observed with 5′-tailed duplex) with the 33mer strand (Figure 5A). In fact, there appeared only very marginal, if at all, hypersensitivity, reflecting a poor binding mode. Moreover, the 61mer strand showed no change in the DNase I pattern until midway through the Rad52 titration (about 1.5 μM), following which there was a large scale protection to DNase I rather than hypersensitivity (above 1.5 μM) (Figure 5B). In this range of protein concentrations, only a lone site most proximal to the 3′ of the strand exhibited a marginal hypersensitivity. The basis of such a mixed pattern is unclear. It was surprising to observe a binding mode of hRad52 on this strand that led to strand protection as opposed to hypersensitivity (see Discussion). Furthermore, the 83mer strand showed only a marginal DNase I sensitivity as a function of hRad52 concentration (Figure 5C). However, there was no indication of any protection against DNase I cleavage even at the highest concentration of hRad52. It appears that even though the 83mer strand length allows a good binding of Rad52 (Figure 4C), the bound DNA does not exhibit a clear signature of hypersensitivity of the type revealed by 121mer and 5′-tailed duplexes. Although the 61- and 83mer strands share the same sequence stretch as the 121mer (Figure 4A) and are proficient in Rad52 binding

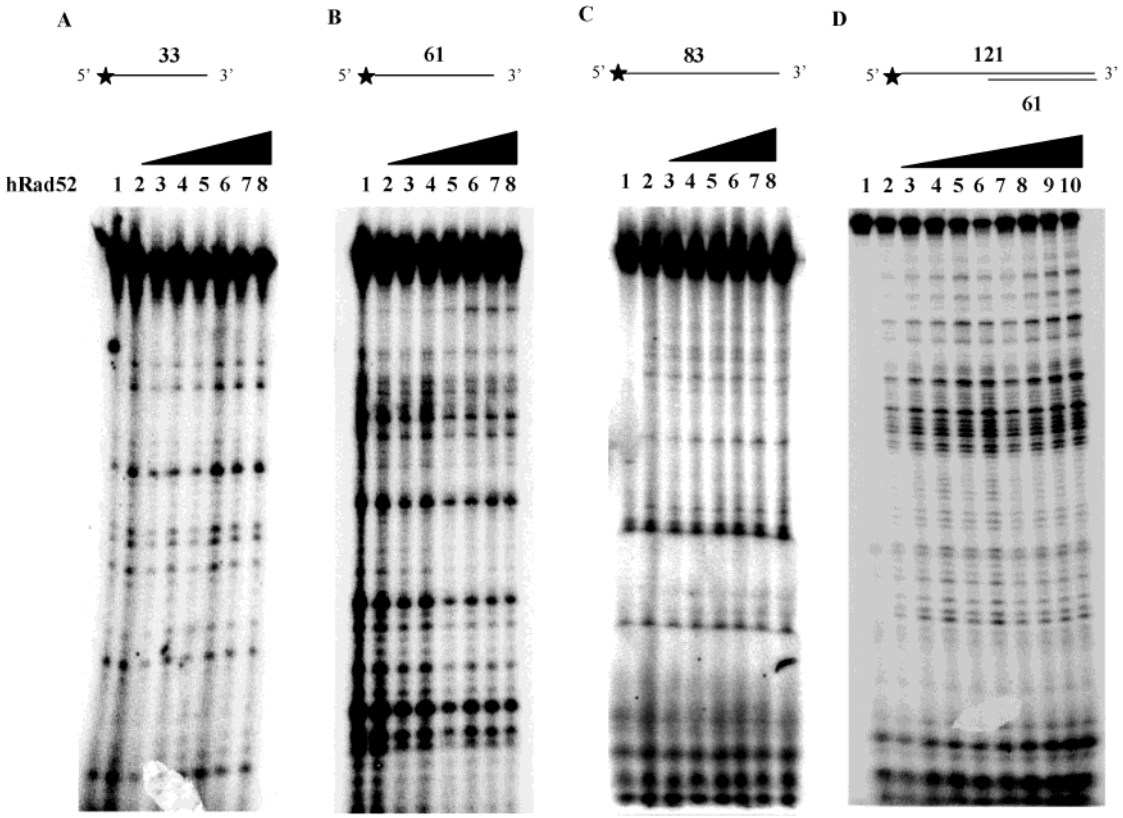

FIGURE 5: ssDNA length dependence of hRad52 binding: DNaseI probing assay. (A) ^{32}P labeled W58C ssDNA (1.0 μM) or (B) ^{32}P labeled Gce ssDNA (1.0 μM) or (C) ^{32}P labeled W78 (1.0 μM) or (D) ^{32}P labeled CLL annealed with unlabeled complementary 5T-CLL (1.0 μM, double-tailed duplex) were incubated with increasing concentrations of hRad52, followed by DNase I probing analyses (0.325 ng/μL for ssDNA and double-tailed duplex and 0.16 ng/μL for dsDNA) (see Materials and Methods). Lane 1 in panel D contains the sample where neither hRad52 nor DNase I was added. The samples in all the remaining lanes were DNase I treated. In panels A−C, lanes 1−8 contain 0, 0.5, 1.0, 1.5, 2.0, 2.5, 3.0, and 3.5 μM hRad52, respectively. In panel D, lanes 2−10 contain 0, 0.5, 1.0, 1.5, 2.0, 2.5, 3.0, 3.5, and 4.0 μM hRad52, respectively.

(Figure 4C), these targets seem to generate complexes where the DNA is not in hypersensitive state, suggesting the possibility of heterogeneity in Rad52−DNA complexes (see Discussion).

hRad52 Promotes Homologous Pairing between ssDNA and the Linear Duplex DNA (Three-Stranded DNA Pairing). In the preceding experiments, it became clear that hRad52 has a distinct binding preference to ssDNA as compared to that of dsDNA. To understand the significance of such a binding preference, we tested whether ssDNA coated with hRad52 can show homologous pairing with a dsDNA. Encouraged by the findings that in vivo yeast Rad52 protein does mediate homology based DNA repair events, even in the absence of Rad51, we tested the competence of hRad52 in facilitating three-stranded pairing on its own. Unlike the reported D-loop products, which involve hRad52 mediated pairing between single strand and supercoiled duplex (*27*−*29*), in this study we have monitored three-stranded pairing involving a linear dsDNA (see Discussion).

GCL ssDNA (121mer) was incubated with an increasing concentration of hRad52 followed by the addition of the labeled homologous duplex DNA (GCL:CLL duplex, 121 bp). It is to be noted that the same strand that functioned as the filament strand (GCL, W strand in the cartoon diagram, Figure 6A) was labeled in the duplex DNA. The level of three-stranded DNA complexes formed was assessed by either a gel assay or a filter-binding assay. As in the gel-retardation assay, the complexes formed in this pairing assay were also fixed by glutaraldehyde prior to scoring (Figure 6A). As a heterologous control, we used a PUC strand (121mer) coated with hRad52 followed by pairing with labeled duplex DNA (GCL:CLL duplex, 121 bp). The labeled duplex DNA was free of any contaminating single strands, and the heterologous PUC strand was as competent in binding hRad52 as the homologous GCL strand (data not shown).

Gel Assay. A side-by-side comparison of homologous versus heterologous reactions revealed that a measurable level of labeled duplex DNA was gel retarded specifically in the homologous set. The extent of the gel-retarded signal was not only homology but also protein concentration dependent (Figure 6B). Although the pairing was homology dependent, the signal strength was rather poor; therefore, we corroborated this result using an independent assay.

Nitrocellulose Filter-Binding Assay. In this assay, the pairing samples were passed through a set of double filters, where the top filter (nitrocellulose) retains labeled DNA−protein complexes followed by the bottom filter (DEAE membrane) that retains the free (unbound) labeled DNA. Filtration being a quicker method of separating the paired DNA−protein complexes from that of free DNA as compared to that of gel-electrophoretic separation, we surmised that the extent of homologous complexes recovered might be higher. Indeed, this was so (Figure 6C). We observed a markedly higher level of homology dependent paired DNA−protein complexes on the top filter. Moreover, in the

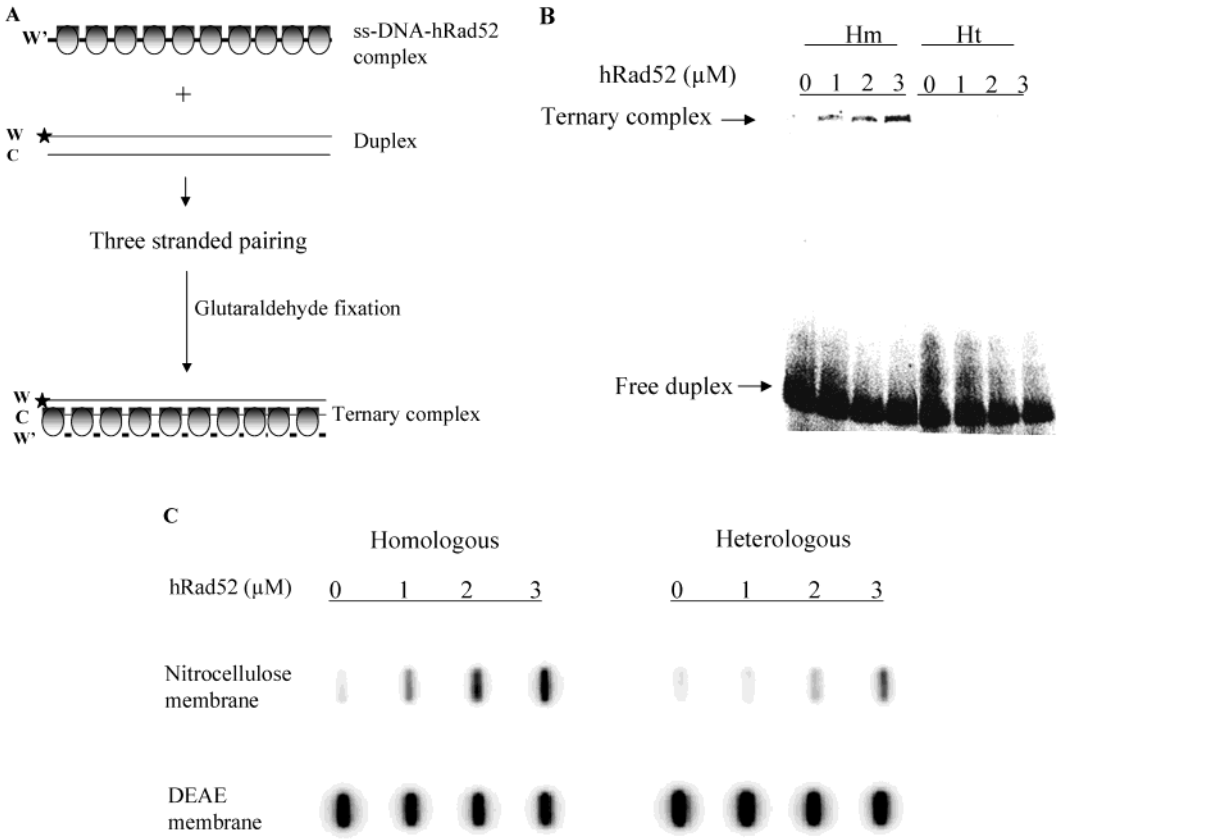

FIGURE 6: Three-stranded pairing assay. (A) A schematic of the pairing assay. ssDNA−hRad52 complex is formed by incubating either GCL (2.0 μM) (homologous) or PUC strands (2.0 μM) (heterologous) with increasing levels of hRad52 (line represents ssDNA and the shaded ovals depict hRad52 oligomers). The labeled duplex DNA, made by annealing ^{32}P labeled GCL with unlabeled CLL (1.0 μM each), was added to ssDNA−hRad52, followed by raising $MgCl_2$ concentration (10 mM) to initiate three-stranded pairing. After an incubation at 37 °C for 10 min, the samples were fixed with 0.2% glutaraldehyde to generate the ternary complexes. Half of the sample was subjected to analyses by native PAGE and the other half were passed through a double-filter setup (KOH treated nitrocellulose membrane on top and DE-50 membrane at the bottom) as described in the Materials and Methods. (B) The dried native gel and (C) the filter membranes from the experiment were autoradiographed. Radioactivity associated with ternary complexes and the free duplex DNA are indicated (B). Similarly, the radioactivity retained on top nitrocellulose and bottom DEAE membranes are indicated in each set against the corresponding protein concentration (C).

homologous set, the radioactive signal increased on the nitrocellulose filter as a function of protein concentration and led to a concomitant drop of the signal on the DEAE membrane. Quantitation revealed that about 30−40% of labeled duplex was converted into three-stranded complexes at the highest protein concentration in the homologous set, whereas the nonspecific signal in the heterologous control reached about a 10% level. Therefore, this assay result suggested that the mobility-retarded DNA signal in the gel assay represented a genuine pairing reaction involving specific three-stranded complexes. Encouraged by the recovery of a reasonable signal of three-stranded pairing, we tested whether any strand exchange activity was associated with these complexes. We did this by scoring the release of labeled single strands (W-strand in the duplex, Figure 6A) following the deproteinization of three-stranded complexes. However, gel analysis showed no traces of any displaced strand either in the homologous or in the heterologous set (data not shown). Even at the highest protein concentration, there was no indication of any strand displacement.

These results suggest that the hRad52 protein is simply capable of facilitating a homologous alignment of three strands, which do not progress toward strand exchange. The DNA length associated with these putative three-stranded complexes was 121 bases. We wondered whether this length posed a barrier for strand exchange but not to strand pairing. If this were so, a shorter homology length might reveal strand exchange products as well as three-stranded pairing. We tested this proposition in following experiments.

Three-Stranded Pairing versus Strand Exchange. We had shown earlier that hRad52 can efficiently bind a 61mer ssDNA (Gce) (Figure 4C). Therefore, we performed three-stranded pairing using oligonucleotides of this length. To test whether three-stranded pairing associated with the AT-rich type of weaker duplexes leads to some level of strand exchange, an A60:T60 duplex was also compared. A binding assay with A60 as a function of the hRad52 concentration revealed that A60 was as good a target for hRad52 binding as Gce. Essentially all the DNA was converted into gel-shifted complexes when about 1−2 μM hRad52 was added to either single strand (data not shown). An A-repeat (A60) and mixed sequence (Gce) single strands were separately incubated with an increasing level of hRad52 followed by pairing with ^{32}P labeled A60:T60 and Gce:Cle homologous duplex DNA, respectively. In both duplexes, the filament strands (i.e., A60 and Gce) were labeled. Therefore, in this design, one can score strand exchange by assessing the level of the displaced single strand from the duplex DNA. The labeled duplexes were free of any contaminating single strands. As heterologous controls, we swapped the labeled

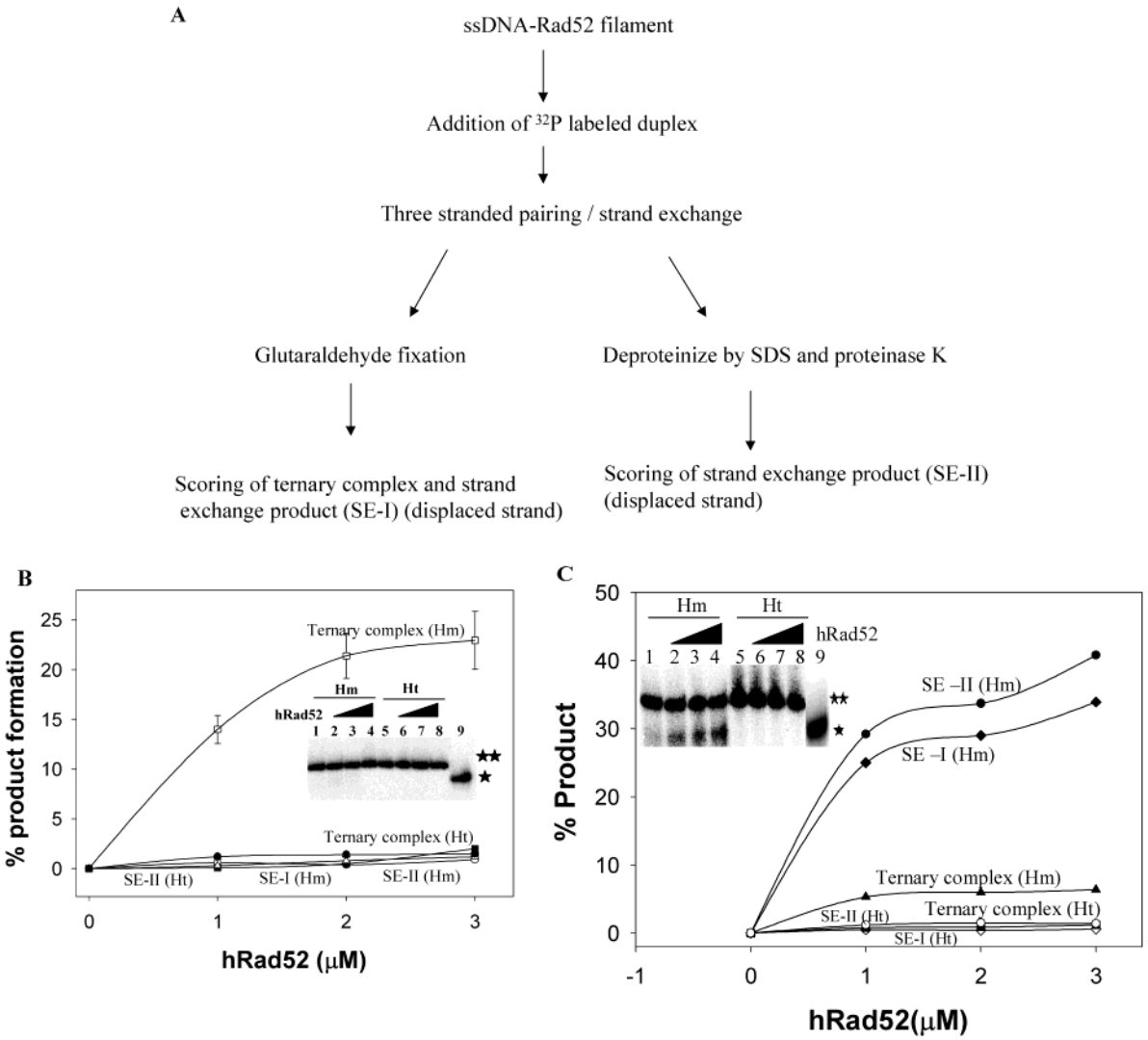

FIGURE 7: Relationship between three-stranded pairing and DNA strand exchange mediated by hRad52. (A) A flowchart of the assay. ssDNA−hRad52 complex was formed by incubating Gce (2.0 μM) (corresponding to homologous, Hm) or A60 (2.0 μM) (corresponding to heterologous, Ht) with an increasing level of hRad52 (0, 1.0, 2.0, and 3.0 μM) (Materials and Methods). Pairing and strand exchange was initiated by adding labeled duplex DNA (generated by annealing labeled Gce with unlabeled Cle strands) (1.0 μM each) and raising the $MgCl_2$ concentration to 10 mM (Materials and Methods). Half of the reaction mixture was fixed with glutaraldehyde, and the other half was deproteinized, followed by analyses on native PAGE. From the gel analyses of glutaraldehyde fixed samples, radioactivity associated with ternary complexes and displaced free Gce strands (SE-I) (if any) are expressed as a percentage of total in each lane. Similarly, radioactivity associated with displaced free Gce strands (SE-II) is quantified from deproteinized strand exchange samples. (B) Ternary complexes in Hm-set (open squares), ternary complexes in Ht-set (filled circles), SE-II in Hm-set (filled squares), SE-II in Ht-set (open circles), and SE-I in Hm-set (open triangles) are plotted as percentage of total radioactivity in each lane against hRad52 concentration. The inset shows the gel image of the deprotenized samples (lanes 1−4 and 5−8 correspond to 0, 1.0, 2.0, and 3.0 μM hRad52, respectively, and lane 9 contains labeled Gce as ssDNA marker). (C) A60 (2 μM) (corresponding to lanes 1−4) or Cle (2 μM) (corresponding to lanes 5−8) was incubated with 0, 1.0, 2.0, and 3.0 μM hRad52 (lane 9 contains labeled A60 as ssDNA marker). Repeat duplex (labeled A60 annealed with unlabeled T60, 1 μM each) was used to initiate the pairing and strand exchange. SE-I in Hm set (filled diamond), SE-II in Hm set (filled circles), ternary complexes in Hm set (filled triangles), ternary complexes in Ht set (open circles), SE-I in Ht set (open diamond), and SE-II in Ht set (filled squares). The inset shows the gel image of deprotenized samples. The position of duplex DNA is indicated by (★★) and that of ssDNA by (★).

Gce:Cle and A60:T60 duplexes against A60 and Gce filaments, respectively. As described earlier, three-stranded pairing was scored by monitoring paired DNA−hRad52 complexes in the gel assay following glutaraldehyde fixation. In this assay, any appearance of a labeled displaced strand even prior to deprotenization (SE-I in Figure 7A) might reveal complete strand exchange and protein dissociation that are imminent with the pairing reaction. On the other hand, strand displacement that follows only after the steps of deproteinization (SE-II, Figure 7A) might reflect a state where strand exchange/protein dissociation has not gone to completion yet (*35*). To score the SE-II products, samples were deproteinized without prior glutaraldehyde fixation, followed by gel analysis. Quantitation of the gel data revealed that the 61mer mixed sequence duplex (Gce:Cle) exhibited a homology dependent and hRad52 concentration dependent three-stranded pairing (ternary complex-Hm) that released no displaced strands either prior to (SE-I) (Figure 7B) or following deproteinization (SE-II) (inset Figure 7B). With the same duplex, a heterologous filament showed neither pairing nor strand exchange (Figure 7B). The three-stranded pairing was highly homology dependent, and the overall

efficiency was higher than that observed with the 121mer system described earlier (Figure 6B). In the same experiment, three-stranded pairing involving the A60:T60 duplex revealed interesting differences. As compared to that of the Gce:Cle duplex, a smaller fraction of the A60:T60 duplex was recovered as three-stranded complexes (ternary complex-Hm), and concomitantly, a high level of strand displacement (SE-I) was observed even without deproteinization (Figure 7C). Interestingly, the sum of the ternary complexes and SE-I in this reaction almost equaled the level of homologous ternary complexes observed with the Gce:Cle duplex (Figure 7B). A parallel control, where the same duplex reacted with a heterologous filament, yielded neither three-stranded complexes nor strand exchange products. Expectedly, all the homologous deproteinized samples revealed a higher level of strand exchange products (SE-II) (inset, Figure 7C). Again, the heterologous control showed no traces of any strand exchange. It appears that as compared to the mixed sequence strands, homologous pairing between A strand and AT duplex leads to three-stranded complexes that have an easier propensity to go through strand exchange (see Discussion). This was not a protein independent spontaneous effect as it was highly hRad52 concentration dependent.

All these radioactive assays put together suggest that the hRad52 protein has the ability to bind ssDNA efficiently and bring about a homologous pairing with the interacting linear duplex DNA via a three-stranded DNA pathway. It is relevant to point out that unlike the D-loop complexes that are reported earlier (*28*), the three-stranded complexes observed in the current study are not sustained by the intrinsic unpairing of the type associated with the negative superhelicity of the plasmid that the hRad52−ssDNA complex uses for pairing. We were therefore intrigued as to whether the hRad52−ssDNA complex that is homologously paired with the linear duplex can actively unpair the interacting duplex during the act of homology register. To address this issue, we did the following studies with the DNA containing a fluorescence reporter that is sensitive to the level of DNA unpairing.

hRad52 Mediated Strand Pairing as Measured by Changes in DNA Fluorescence. 2-Amino purine (2AP) is a fluorescent analogue of adenine residues and an excellent reporter of conformational changes in DNA. In the current study, an A60 strand with a centrally placed 2AP residue (2AP-A60) was incubated with increasing levels of hRad52 followed by the addition of an equimolar level of complementary T strand (T60). Fluorescence emission at 370 nm following an excitation at 310 nm was measured as a function of time at each protein concentration. We observed a time as well as a protein concentration dependent quenching of fluorescence specifically in the homologous reaction (Figure 8A). Under these conditions, hardly any spontaneous annealing ensued between 2AP-A60 and T60 strands as evidenced by no significant time dependent quenching of 2AP (minus protein control, Figure 8A). We normalized the recovered fluorescence taking the initial counts (at T_0, where T60 was not added) associated with the filament as 100%, and the following trend emerged. At subsaturating levels of protein (1−5 μM), only partial annealing was observed within the time points tested. Only at a high concentration of protein (10 μM), annealing went to near completion approaching the level expected of a fully annealed duplex standard (indicated by the broken line in the Figure 8A). This experiment showed that 2AP fluorescence can be used as a bona fide reporter of DNA pairing even in the presence of protein.

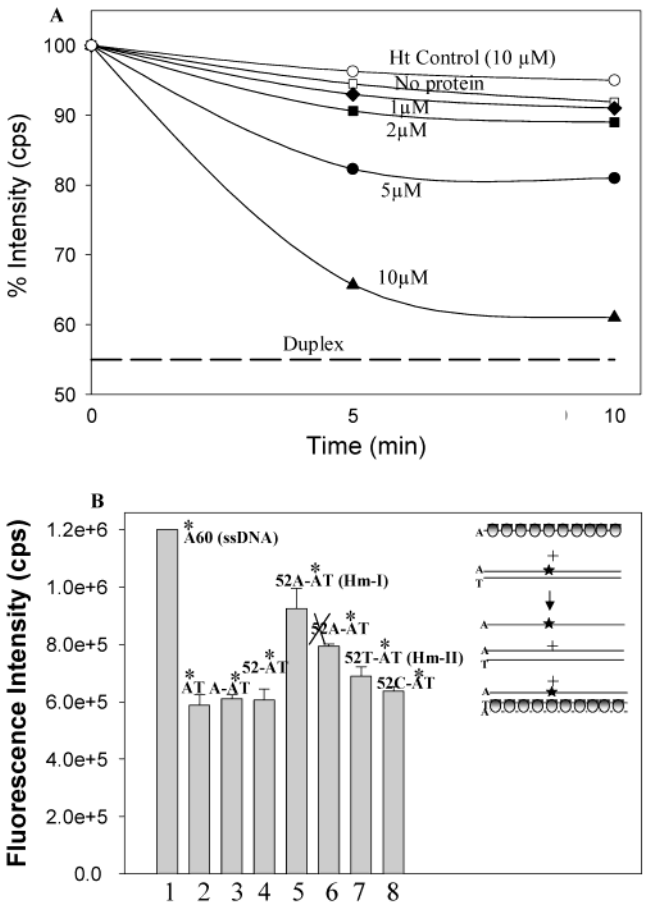

FIGURE 8: (A) ssDNA annealing by hRad52. 2AP-A60 (10 μM) was incubated with varying concentrations of hRad52, followed by the initiation of annealing with complementary strand T60 (10 μM). The samples were excited at 310 nm, and emission at 370 nm was recorded at different time points of annealing. In all these reactions, the starting fluorescence associated with unannealed 2AP-A60 was considered as 100%, with respect to which the percentage quench in annealing is expressed as a function of time. 2AP-A60 (10 μM) incubated with hRad52 (10 μM) was annealed with Gce (10 μM) as a heterologous control (open circles). The horizontal broken line represents the fluorescence quench level of the preformed thermally annealed duplex between 2AP-A60 and T60. (B) Fluorescence changes associated with homology dependent pairing and strand exchange in 2AP-A60:T60 repeat duplex. The star in the inset (schematic of the assay) and asterisk in the figure represents 2AP in all the DNA substrates. Repeat duplex (AT) was made by annealing 2AP-A60 with T60 (10 μM each). (1) A60, ssDNA; (2) AT duplex; (3) naked A60 (10 μM) paired with the AT-duplex (no protein control); (4) hRad52 (10 μM) added to AT duplex; (5) A60 (10 μM) incubated with hRad52 (10 μM), followed by pairing with the AT duplex (homologous-I); (6) sample 5 following proteinase K treatment; (7) T60 (10 μM) incubated with hRad52 (10 μM), followed by pairing with the AT duplex (homologous-II); and (8) Gce (10 μM) incubated with hRad52 (10 μM), followed by pairing with the AT duplex (heterologous). All the pairing reactions were done for 10 min, followed by fluorescence measurements.

In the experiments described next, we studied whether the duplex fluorescence changes as a consequence of three-stranded pairing, and more specifically, whether duplex DNA involved in such pairing undergoes strand unpairing. Two types of A−T repeat duplexes (containing a single 2AP) were tested. In the first set, A60 strand coated with hRad52 was paired with 2AP-A60:T60 duplex followed by measurement

of steady state changes in the fluorescence. In the second set, instead of the entire length of the substrate strand, only the central cassette contained the A-repeat with a single 2AP in the middle, and such a cassette was flanked on either side by mixed sequences (2AP A-template/T-template duplex).

Fluorescence Changes Associated with A60-2APA60:T60 Three-Stranded Complexes. A single 2AP containing duplex (2AP-A60:T60) was prepared by annealing the 2AP-A60 strand with T60. As expected from the previous experiment (Figure 8A), the duplexing of 2AP-A60 resulted in about 50% quenching of the fluorescence, and the ^{32}P end labeling of an aliquot of this mixture followed by native PAGE analysis revealed that it contained no traces of left over single strands (data not shown). In three separate parallel reactions, we incubated this fluorescent duplex with different ssDNA−hRad52 complexes. An A60−hRad52 and T60−hRad52 complex belonged to the homologous set (Hm-I and Hm-II, respectively), whereas that of Cle-hRad52 belonged to the heterologous combination. Under these conditions of filament formation, we made sure that all the three single strands (10 μM each) were efficiently coated with hRad52 protein (10 μM) as assessed by gel-shift analysis of a small labeled aliquot (data not shown). Addition of fluorescent duplex substrate to each of these three filaments, followed by a pairing step, led to interesting changes in the steady state level of fluorescence counts. Only the reaction where an A60 strand paired with the duplex showed significant enhancement in the fluorescence counts (∼50−60%) (52A-AT in Figure 8B). The control where hRad52 was not added (A-AT bar) revealed no changes in the fluorescence signal, suggesting that the observed enhancement in the fluorescence was highly hRad52 dependent. Interestingly, the other homologous control that involved the pairing of the T60−hRad52 complex with the same duplex showed only a negligible level of fluorescence enhancement (52T-AT bar). The third control that involved heterologous pairing with Cle-hRad52 showed no change in the fluorescence counts (52C-AT bar). Another control where we selectively omitted ssDNA but retained all other components of the three-stranded pairing reaction also revealed no measurable change in the fluorescence counts associated with the duplex (52-AT bar). All these controls put together suggest that only the reaction where hRad52 mediates a homologous pairing between an A60 and the 2AP containing the AT repeat duplex leads to the fluorescence enhancement. Such an effect is consistent with the gel-assay results described earlier (Figure 7C) where the reaction had shown signatures of three-stranded pairing (ternary complex, Figure 7C) as well as strand exchange (SE-I, Figure 7C). The enhanced fluorescence in the reaction could stem either from the combined effect of pairing and strand exchange or from strand exchange alone. It is conceivable that a three-stranded complex that has not undergone strand exchange will revert to the starting substrates following the steps of deproteinization (*35*). On the other hand, the same treatment will generate strand exchange products if the pairing was followed by an exchange of strands. To evaluate the relative contributions of these two states in fluorescence enhancement observed, we analyzed the effect of deproteinization in an A60−hRad52 mediated three-stranded complex (i.e., on the 52A-AT set). Following deproteinization, about half of the enhanced fluorescence associated with three-stranded pairing

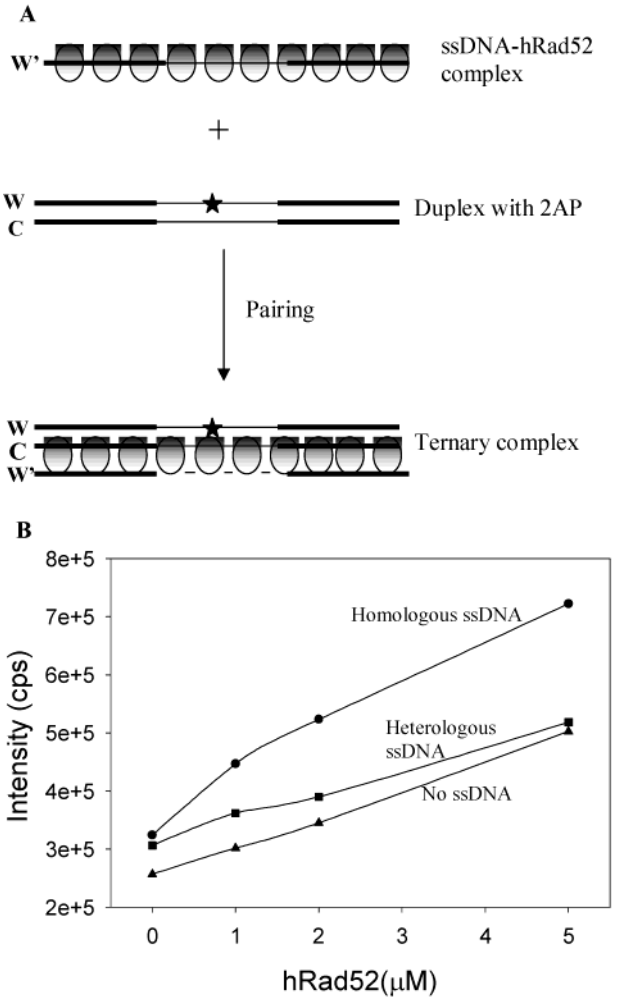

FIGURE 9: Fluorescence changes associated with homology dependent pairing in mixed sequences. (A) Schematic representation of the assay. The ssDNA substrate has a 33mer A-repeat (thin line) in the middle, flanked by mixed sequences (bold lines) on either sides. Duplex substrate is fully homologous to it where a middle A residue is replaced by 2AP (indicated by star). (B) A template (10 μM) was incubated with increasing concentrations of hRad52, followed by the initiation of pairing with a homologous duplex (generated by annealing 2AP-A template with T template, 10 μM each) and the measurement of fluorescence emission after an incubation of 10 min (Materials and Methods). In parallel, two controls were performed: heterologous control where Cle was used instead of A template and a minus ssDNA control where neither A-template nor Cle was used. The fluorescence intensities recovered at 370 nm were plotted against hRad52 concentration. Homologous (filled circles), heterologous (filled squares), and minus ssDNA control (filled triangles).

was quenched (crossed 52A-AT bar), which suggested that a measurable fraction of fluorescence enhancement stemmed from the reversible category, namely, that of a configuration where the strands had not switched (see Discussion). If this were so, the protein might mediate homologous pairing of a single-strand with that of its duplex through a mechanism that involves transient unpairing of duplex, which we tested more rigorously in the following experiment.

In this assay, we studied an AT repeat duplex that is flanked on either side by mixed sequences (Figure 9A). It is to be noted that while the former substrate design (A60-A60:T60) brings about a three-stranded pairing that is imminent with strand exchange (Figures 7C and 8B), the present one is unlikely to lead to strand exchange based on

the findings that a 61mer mixed sequence duplex (Gce:Cle) upon pairing with homologous ssDNA had led to no strand exchange products (Figure 7B). Moreover, one of the possibilities of an artifactual effect of strand exchange arising due to branch-migration related events in A60:T60 duplexes (in former design) can be minimized in the present duplex where mixed sequences flank the AT repeats (see Discussion). Therefore, such a variation in duplex design (as shown in Figure 9A) allows us to monitor 2AP-fluorescence changes in the same sequence context as that of A60:T60 duplex, but without the associated effects of strand exchange. Thereby, it facilitates an accurate comparison of homologous duplex unpairing in a setting where pairing is associated with strand exchange (as in former design, Figure 8B) vis-à-vis that without strand exchange (as in the current one, Figure 9A). To correlate the fluorescence results more closely with that of the radioactive pairing assays, in this experiment we monitored fluorescence changes as a function of hRad52 concentration. Homologous (A-template) and heterologous strands (Cle) were separately incubated with an increasing concentration of hRad52 followed by pairing with 2AP containing duplex (2AP A-template:T-template) and measurement of steady state level of fluorescence. Another parallel control included a set identical to that of homologous/heterologous reaction but without the ssDNA. Expectedly, in the set where no protein was added, the fluorescence level of a naked 2AP-duplex in the three reactions was essentially similar (Figure 9B). In the control that contained only the 2AP-duplex (i.e., minus ssDNA control), there was a protein concentration dependent increase in the fluorescence, and the heterologous reaction essentially mimicked the same trend. It is possible that the marginal binding of hRad52 with the duplex might itself lead to some increase in fluorescence, the trend of which was visible even with the A60:T60 duplex (data not given), although the percent increase there was less as compared to that of the 2AP A-template:T-template duplex observed here. It is not clear how hRad52 binding itself affects duplex fluorescence and how duplex sequence context effects influence the fluorescence emission levels. Notwithstanding this caveat, we observed that a homologous pairing reaction showed a markedly higher fluorescence level than that of either the heterologous or minus ssDNA set at every concentration of hRad52 tested (Figure 9B). The percentage enhancement in the fluorescence counts associated with homologous reaction at the highest concentration of protein was highly comparable to that observed with 2AP A60:T60 duplex system described earlier. It is pertinent to point out that just as the 2AP-A60 strand (Figure 8A), the 2AP-A-template also led to a fluorescence quenching to half its starting level following annealing with the T-template (data not shown), suggesting that about a 100% rise in fluorescence counts associated duplex unpairing reflects a configuration similar to strand separation. Therefore, the high extent of fluorescence enhancement that is specifically associated with the homologous pairing set reveals that base pairs in the 2AP-template duplex seem to undergo a significant level of unpairing during homologous alignment (see Discussion). Consistent with this interpretation was the observation where in a reciprocal control, an incoming 2AP containing ssDNA (2AP-A60 or 2AP-A-template) exhibited fluorescence quenching following its pairing specifically with its homologous duplex (non-2AP containing) (A60:T60 and A-template:T-template, respectively) that was entirely hRad52 dependent (data not shown).

DISCUSSION

Molecular genetic studies have clearly demonstrated that yeast Rad52 serves an essential role in homologous recombination, where some pathways are Rad51 dependent and some are not (*4*). The precise molecular basis of this dichotomy is far from clear. Not withstanding the belief that mammalian and other higher eukaryotic Rad52 may not be as essential as that of yeast (*36*), it is clear that Rad52 plays an important role in maintaining genomic stability in these cells. Biochemical studies have demonstrated that hRad52 binds ssDNA and catalyzes strand annealing as well as pairing between single strands and supercoiled duplexes generating D-loop complexes (*27*−*29*). In this study, we have made an attempt to clarify the relative binding ability of hRad52 with single versus double strands, to denote the DNA length dependence, and to describe a a novel facet of three-stranded pairing, the features of which are discussed next.

Data from electron microscopic image reconstruction studies as well as a high-resolution crystal structure of the hRad52 protein points out that it oligomerizes into a ring shaped complex containing either seven monomers (of full-length protein) (*7*) or 11 monomers (of C-terminally deleted protein) (*29*, *30*). Interestingly, an 11-membered ring seems to be as active as the seven-membered ring in the biochemical functions tested, suggesting that the high-resolution structural information derived from the 11-membered ring may be relevant to the full-length protein oligomers as well. One of the most interesting features of the structural information was the suggestion that the DNA binding groove houses clusters of amino acid residues that are shared by both single- and double-stranded DNA binding, a hallmark of a composite binding site. It also turns out that the groove where the DNA target was modeled in the protein structure is too narrow to accommodate duplex DNA without invoking a conformational change. It is this notion that provoked us to look at the conformational status of the duplex that is part of homologously aligned three-stranded complex in the hRad52 system.

We found that the protein stably binds to ssDNA targets, thereby generating distinct and highly mobility-retarded hRad52−DNA complexes (Figure 2). A binding comparison revealed that single-stranded DNA is a much more preferred target than the duplex DNA (Figure 3), where 5′- versus 3′-tails performed equally well (data not shown). The protein seems to show a preference for binding single strands that are at least as long as 61−121mers. A minimum of about 30 bases may be required to encompass a given seven-membered ring, if we assume a binding site of four bases/monomer (*30*). Perhaps Rad52 complexes formed with shorter ssDNA targets may not be stable enough to survive gel-shift analyses, and more carefully designed solution phase equilibrium binding studies are needed to address the issues related to Rad52−ssDNA stability versus the length of ssDNA targets. As predicted from the structure as well as hydroxyl radical cleavage studies (*30, 37*), the ssDNA complexed with the ring should be accessible from outside. This is also supported by our DNase I results where it was seen that the 121mer strand and tailed duplexes were

rendered highly sensitive to the nucleolytic attack following complexation with the protein (Figure 1). However, 61- and 83mer targets that bind Rad52 well did not exhibit enhanced sensitivity to DNase I cleavages (Figure *5*). In fact, the 61mer strand largely exhibited nuclease protection following Rad52 binding. It is therefore unclear whether such alterations in the nuclease sensitivity status of bound DNA targets reflect an underlying structural heterogeneity in various protein−DNA complexes. It is tempting to speculate that hRad52 protein rings in the protein−DNA complexes may have the propensity to break, thereby transforming part of the complex into a helical form where now the bound DNA may locate toward the interior of the helical filament. Electron microscopic images have revealed the presence of broken rings in Rad52 protein preparations (*38*), and the plausibility of such a structural transformation from a ring form to a filament form has been elegantly described for β-protein of bacteriophage λ, a functional homologue of hRad52 (*9*). Notwithstanding such interesting possibilities, currently, available information about the details of the DNA path in Rad52−ssDNA complexes is too sketchy; therefore, we cannot fully rationalize a lack of DNase I sensitivity effects observed with 61- and 83mer strands.

The periodicity of cleavage that was observed with the hydroxyl radical approach was not at all evident in DNase I cleavage experiments where the strand was rendered hypersensitive (Figure 1). The reason for such a discrepancy is not clear. In fact, one has to note that the reported hydroxyl radical cleavage 4*n* repeat pattern seems to require single strands whose length is a multiple of 4 nucleotides, suggesting that the observed periodicity is related to an interesting facet of Rad52 binding where the protein is precisely phased with respect to the target ssDNA ends (*37*). On the contrary, the target lengths chosen in the current study were not multiples of 4 nucleotide units and may not have led to a precise 4*n* repeat pattern in the hydroxyl radical cleavage experiment. Therefore, the DNase I cleavage pattern observed in the current study cannot be directly compared with the reported hydroxyl radical cleavage pattern. However, if one assumes that the accentuated cleavages observed in DNase I as well as the hydroxyl radical approaches the stem from the distorted backbone of ssDNA held closely by the opposing binding surface of the protein, it is conceivable that the bases may be relatively freely displayed outward away from the protein contacts. In fact, analyses of motional dynamics of 2AP base in Rad52−DNA complexes using a fluorescence approach strongly supports such a model (unpublished observations). This model is highly congenial to conceptualize how the protein might facilitate annealing of the bases with the incoming complementary base. A somewhat similar model can also rationalize the formation of D-loops where annealing involves a nascent single strand associated with a supercoiled duplex. However, on the basis of the results described here, we believe that the protein is capable of achieving not only annealing but also a three-stranded DNA pairing. The radioactive assays revealed that linear duplex substrate comigrates (native PAGE assay) as well as coretains (nitrocellulose filter assay) with the ssDNA−hRad52 complexes in a homology dependent manner (Figure 6). The complexes were entirely sustained by the presence of protein, a hallmark of true ternary complexes where the single and double strands cross-talk with each other only on the protein surface. When the homologously aligned sequences were of mixed sequence type (nonrepeats), such ternary complexes did not reveal any exchange of strands (i.e., strand displacement was observed neither in the ternary complexes nor following deproteinization (Figure 7B)). However, if the three-stranded pairing involved the A60:T60 duplex, strand displacement was evident even prior to deproteinization (Figure 7C). This result suggested an interesting possibility where the protein might unwind the duplex in the ternary complex during the homology readout, which in a weaker duplex such as the A-repeat:T-repeat leads to the displacement of the strand in the gel assay. We tested this possibility using a fluorescence assay where 2AP (2-amino purine) served as an excellent reporter of transient unpairing in the duplex.

2AP is a bona fide structural analogue of adenine residues in DNA. The fluorescence yield of 2AP is highly sensitive to the conformational state of the duplex it is in and hence has been widely used as a good reporter for duplex unwinding (*34*, *39*−*41*). We had earlier used 2AP to monitor RecA mediated unwinding of A60:T60 duplexes (*34*). Since the fluorescence quantum yield of 2AP in the DNA strand is highly sequence context dependent (*42*), we used 2AP within a cassette of theA60:T60 duplex, where a single adenine was substituted with a 2AP. The quantum yield of such duplexes was high enough to monitor the changes associated with DNA unpairing confidently. In such a substrate setting, complete annealing of the 2AP strand by its complement led to nearly 50% quenching of fluorescence (Figure 8A), which amounted to the fluorescence yield depletion of about 0.6 million cps (as s/r) (Figure 8B), a sufficiently high count to study changes associated with an even partial unpairing of duplexes. As expected, 2AP containing a single strand coated with hRad52 exhibited a protein concentration as well as a time dependent quenching of fluorescence to a level of duplex DNA, following the addition of the complementary strand (Figure 8A). This assured that DNA related changes (annealing in this case) could be easily monitored even in the presence of the protein. The A60:T60 duplex that had revealed strand displacement of ternary complexes in a radioactive gel assay (Figure 7C) exhibited a nearly 50−60% increase in its fluorescence following pairing (Hm-I) (52A-AT bar in Figure 8B). The increase in fluorescence was dependent on hRad52 protein mediated homologous pairing. Interestingly, the enhanced fluorescence associated with such three-stranded pairing was partially lost following deproteinization. This suggested that duplex unpairing as well as strand displacement were the likely causes of fluorescence increase, out of which only the former was reversed by the deprotenization treatment. The fluorescence and radioactive assay results were consistent with each other and strongly hinted at the possibility of duplex unpairing in homologous ternary complexes. Another homologous reaction involving T-repeat as an incoming strand (Hm-II) behaved differently where the addition of the 2AP duplex led to a negligible enhancement in the fluorescence signal (compare 52T-AT bar with that of 52A-AT bar in Figure 8B). As expected, this contrast strongly suggests that only in the Hm-I configuration will the the 2AP strand of the duplex be in an exit mode due to duplex unpairing as well as strand exchange. In the configuration where the T strand is incoming, the 2AP strand has no opportunity to

attain partial single strandedness since it may be in a rapid equilibrium with either T strands in the homologous three-stranded complex. We reconfirmed these transient unpairing related fluorescence changes in a more stringent substrate setting, where the homologous duplex could not go past three-stranded pairing into strand exchange phase. This design was based on our earlier finding that the hRad52 protein catalyzed the formation of homologously paired ternary complex that did not undergo strand exchange in a mixed sequence setting (Figure 7B). Such a reaction provided a more definitive way of testing transient unpairing associated with the duplex, which does not lead to extensive strand separation due to exchange. Interestingly, even in such a setting, we observed a distinct fluorescence increase that was homology dependent as well as protein dependent (Figure 9B). The fluorescence increase was markedly higher in homologous three-stranded complexes than the equivalent heterologous controls. Since the highly sensitive radioactive assays did not reveal any indication of strand displacement in these complexes (data not shown), the homology dependent increase in the 2AP fluorescence pointed out that the duplexes were undergoing partial and perhaps transient unpairing in the homologous three-stranded pairing.

These results put together allow us to visualize the following important mechanistic insight related to hRad52 mediated three-stranded pairing. The hRad52−ssDNA complex may be endowed with a property through which the incoming duplex DNA is checked for the presence of homology via a three-stranded DNA that involves partial unpairing of the duplex substrate. The protein may accomplish this even without the help of super helical energy in the duplex as shown in the current results. However, since the substrates studied here did not involve a buried homology configuration, we cannot rule out the effect of a two-strand annealing component contributed by the homologous DNA ends in the three-stranded pairing reaction. Nonetheless, it is interesting to note that the protein seems to generate a complex where the three strands are homologously aligned, but the strand exchange is largely uninitiated despite the presence of free ends in the region of homology. Future studies are geared toward trying to understand the relevance of such a complex vis-à-vis its processing by other protein components of the *RAD52* epistasis group. It is also interesting to think about the relevance of such a DNA alignment in the context of the break induced replication model where active and extensive strand exchanges are not required.

ACKNOWLEDGMENT

We thank Prof. Stephen C. West, Cancer Research UK, Clare Hall laboratories UK for kindly providing the overexpression clone of human Rad52; Prof. G. Krishnamoorthy, Department of Chemical Sciences, TIFR, for help in fluorescence experiments; and Sunita Ramanathan and Amita Joshi for their critical input.

REFERENCES

1. Baumann, P., and West, S. C. (1998) *Trends Biol. Sci. 23*, 247−251.
2. Hiom, K. (1999) *Curr. Biol. 9*, 446−448.
3. Haber, J. (2000) *Trends Genet. 16*, 259−264.
4. Pacques, F., and Haber, J. E. (1999) *Microbiol. Mol. Biol. Rev. 63*, 349−404.
5. Shinohara, A., and Ogawa, T. (1995) *Trends Biochem. Sci. 20*, 587−591.
6. Shinohara, A., Shinohara, M., Ohta, H., Matsuda, S., and Ogawa, T. (1998) *Genes Cells 3*, 145−156.
7. Stasiak, A. Z., Larquet, E., Stasiak, A., Muller, S., Engel, A., Van dyck, E., West, S. C., and Egelman, E. H. (2000) *Curr. Biol. 10*, 337−340.
8. Thresher, R. J., Makhov, A. M., Hall, S. D., Kolodner, R., and Griffith, J. D. (1995) *J. Mol. Biol. 254*, 364−371.
9. Passy, S. I., Yu, X., Li, Z., Radding, C. M., and Egelman, E. H. (1999) *Proc. Natl. Acad. Sci. U.S.A. 96*, 4279−4284.
10. Tsukamoto, Y., Kato, J., and Ikeda, H. (1996) *Genetics 142*, 383−391.
11. Hegde, V., and Klein, H. (2000) *Nucleic Acids Res. 28*, 2779−2783.
12. Ricchetti, M., Dujon, B., and Fairhead, C. (2003) *J. Mol. Biol. 328*, 847−862.
13. Shen, Z., Cloud, K. G., Chen, D. J., and Park, M. S. (1996) *J. Biol. Chem. 271*, 148−152.
14. Park, M. S., Ludwig, D. L., Stiggers, E., and Lee, S. H (1996) *J. Biol. Chem. 271*, 18996−19000.
15. Milne, G. T., and Weaver, D. T. (1993) *Genes Dev. 7*, 1755−1765.
16. Jackson, D., Dhar, K., Wahl, J. K., Wold, M. S., and Borgstahl, G. E. O. (2002) *J. Mol. Biol. 321*, 133−148.
17. Liu, Y., and Maizels, N. (2000) *EMBO Reports 1*, 85−90.
18. Benson, F. E., Baumann, P., and West, S. C. (1998) *Nature 391*, 401−404.
19. Shinohara, A., and Ogawa, T. (1998) *Nature 391*, 404−407.
20. New, J. H., Sugiyama, T., Zaitseva, E., and Kowalczykowski, S. C. (1998) *Nature 398*, 407−410.
21. Krejci, L., Song, B., Bussen, W., Rothstein, R., Mortensen, U. H., and Sung, P. (2002) *J. Biol. Chem. 277*, 40132−40141.
22. Sung, P. (1997) *Genes Dev. 11*, 1111−1121.
23. Sugiyama, T., and Kowalczykowski, S. C. (2002) *J. Biol. Chem. 277*, 31663−31672.
24. New, J. H., and Kowalczykowski, S. C. (2002) *J. Biol. Chem. 277*, 26171−26176.
25. Reddy, G., Golub, E. I., and Radding, C. M. (1997) *Mutat. Res. 377*, 53−59.
26. Sugiyama, T., New, J. H., and Kowalczykowski, S. C. (1998) *Proc. Natl. Acad. Sci. U.S.A. 95*, 6049−6054.
27. Kurumizaka, H., Aihara, H., Kagawa, W., Shibata, T., and Yokoyama, S. (1999) *J. Mol. Biol. 291*, 537−548.
28. Kagawa, W., Kurumizaka, H., Ikawa, S., Yokoyama, S., and Shibata, T. (2001) *J. Biol. Chem. 276*, 35201−35208.
29. Kagawa, W., Kurumizaka, H., Ishitani, R., Fukai, S., Nureki, O., Shibata, T., and Yokoyama, S. (2002) *Mol Cell. 10*, 359−371.
30. Singleton, M. R., Wentzell, L. M., Liu, Y., West, S. C., and Wigley, D. B. (2002) *Proc. Natl. Acad. Sci. U.S.A. 99*, 13492−13497.
31. Karthikeyan, G., Wagle, M. W., and Rao, B. J. (1998) *FEBS. Lett. 425*, 45−51.
32. Sambrook, J., Fritsch, E. F., and Maniatis, T. (1989) *Molecular Cloning: A Laboratory manual*, p 11.39, Cold Spring Harbor Laboratory Press, Plainview, NY.
33. Wong, I., and Lohman, T. M. (1993) *Proc. Natl. Acad. Sci. U.S.A. 90*, 5428−5432.
34. Sen, S., Krishnamoorthy, G., and Rao, B. J. (2001) *FEBS Lett. 491*, 289−298.
35. Roselli, W., and Stasiak, A. (1990) *J. Mol. Biol. 216*, 335−352.
36. Sonoda, E., Takata, M., Yamashita, Y. M., Morrison, C., and Takeda, S. (2001) *Proc. Natl. Acad. Sci. U.S.A. 98*, 8388−8394.
37. Parsons, C. A., Baumann, P., Van Dyck, E., and West, S. C. (2000) *EMBO J. 19*, 4175−4181.
38. Van Dyck, E., Hajibagheri, N. M. A., Stasiak, A., and West, S. C. (1998) *J. Mol. Biol. 284*, 1027−1038.
39. Millar, D. P. (1996) *Curr. Opin. Struct. Biol. 6*, 322−326.
40. Lam, W. C., Van der Schans, E. J., Sowers, L. C., and Millar, D. P. (1999) *Biochemistry 38*, 2661−2668.
41. Allan, B. W., Beecham, J. M., Lindstrom, W. M., and Reich, N. O. (1998) *J. Biol. Chem. 273*, 2368−2373.
42. Jean, J. M., and Hall, K. B. (2001) *Proc. Natl. Acad. Sci. U.S.A. 98*, 37−41.

BI0350452